

Biochemical, Cell Biological, and Molecular Dynamics

Studies of the Fission Yeast α -Actinin Ain1

January 2020

Rikuri MORITA

Biochemical, Cell Biological, and Molecular Dynamics

Studies of the Fission Yeast α -Actinin Ain1

A Dissertation Submitted to

the Graduate School of Life and Environmental Sciences, the University of Tsukuba

in Partial Fulfillment of the Requirements

for the Degree of Doctor of Philosophy in Science

(Doctoral Program in Biological Sciences)

Rikuri MORITA

Table of contents

i.	Abstract	1
ii.	Abbreviations	3
iii.	General Introduction	4
iv.	Chapter I	10

Biochemical and cell biological studies of α -actinin Ain1

	Introduction	11
	Materials and Methods	13
	Results	17
	Discussion	24
v.	Chapter II	27

Molecular dynamics study of α -actinin Ain1

	Introduction	28
	Materials and Methods	33
	Results	36
	Discussion	40
vi.	General Conclusion	44
vii.	Acknowledgements	45
viii.	References	46
ix.	Figures	57

i. Abstract

The actin cytoskeleton is involved in various cellular processes, such as crawling on substrates, intracellular transport of vesicles and organelles, cell morphogenesis, and cytokinesis. Actin-binding proteins modulate the structure and function of F-actin in these processes. In particular, actin-bundling proteins bundle F-actin and assemble the three-dimensional meshwork of actin cytoskeleton.

The fission yeast *Schizosaccharomyces pombe* forms a contractile ring (CR) during cytokinesis and utilizes its constriction to guide a septum. Fission yeast has several actin-bundling proteins, although the differences in their function have not yet been fully discovered. Ain1 is the sole homolog of α -actinin in fission yeast and specifically localizes to the CR. It has previously been shown that loss of the *ain1⁺* gene induces cytokinetic defects under stressful conditions.

Here, I studied the biochemical interactions between Ain1 and F-actin and structural mechanism behind their interaction. It was found that Ain1 had a weaker affinity for F-actin than the other actin-bundling proteins. However, microscopy showed that Ain1 was able to bundle F-actin into thick filaments. A point-mutation R216E in the actin-binding domain (ABD), which corresponds to a pathogenic mutation in mammalian α -actinin, enhanced the actin-binding activity of Ain1 and bundled F-actin into a disorderly aggregation.

Next, to characterize the functional domain of Ain1, the cellular localization of truncated and mutated Ain1 was examined. I successfully demonstrated the role-sharing

relationship of the two calponin homology domains in detail. In addition, the C-terminal EF-hand was found to be essential for actin-binding *in vivo* but unnecessary *in vitro*.

In addition, I studied the molecular mechanism of the interaction between Ain1 and F-actin. It had previously been proposed that the R216E mutation in α -actinin promoted the close-open conformational change of the ABD and enhanced its actin-binding activity. To investigate the transition mechanism, molecular dynamics simulations were performed. However, I did not observe the close-open conformational change. My study unexpectedly revealed a novel actin-binding region on Ain1 molecule and a mutation in this region abrogated the cellular localization of Ain1.

In this thesis, I examined the properties of the α -actinin Ain1 by biochemical, cell biological, and molecular dynamics studies.

ii. Abbreviations

ABD,	Actin binding domain
ABS,	Actin binding site
ATP,	Adenosine triphosphate
CH,	Calponin homology
CR,	Contractile ring
DTT,	Dithiothreitol
EDTA,	Ethylenediaminetetraacetic acid
EGTA,	Ethylene glycol tetraacetic acid
EMM,	Edinburgh Minimal Medium
F-actin,	Filamentous actin
G-actin,	Globular actin
GFP,	Green fluorescent protein
GST,	Glutathione-S-transferase
HRP,	Horse radish peroxidase
IPTG,	Isopropyl β -D-thiogalactopyranoside
MD,	Molecular dynamics
NMR,	Nuclear magnetic resonance
PCA,	Principle component analysis
PC,	Principle component
PDB,	Protein data bank
PIP ₂ ,	Phosphatidylinositol 4,5-bisphosphate
PME,	Particle mesh Ewald
PMSF,	Phenylmethylsulfonyl fluoride
PVDF,	Polyvinylidene difluoride
RMSD,	Root mean square deviation
SCPR,	Search, capture, pull, and release
SPR,	Spectrin repeats
YFP,	Yellow fluorescent protein

iii. General Introduction

Cytoskeletons in eukaryotic cells

Elaborate cytoskeletal network are found in various types of eukaryotic cells. There are three major cytoskeletons; actin filament, microtubule, and intermediate filaments.

Microtubules (MTs) are hollow structures assembled from 13 protofilaments consisting of tubulin-heterodimer subunits. MTs engage in chromosomal separation (reviewed by Meunier and Vernos, 2012), ciliary structure formation (reviewed by Loncarek and Bettencourt-Dias, 2017), and axon transport in neurons (reviewed by Conde and Cáceres, 2009). On the contrary, a main role of intermediate filaments (IFs) is to endow an animal cell with mechanical stiffness. IFs line the plasma membrane and attach to cell-cell contact sites and cell-substrate interaction sites (reviewed by Herrmann et al., 2007). In addition, some IFs form a laminar structure beneath the nuclear membrane.

The subunit of Ifs are anti-parallel polymers of filamentous proteins.

Actin cytoskeletons have important roles in not only muscle contraction but also in various cellular processes such as cell division, cell motility, and intracellular transport. The actin subunit is a flat 42 kDa protein with an amino acid sequence that is highly conserved in eukaryotes as well as MTs. Actin binds to an ATP or ADP molecule. Monomeric actins (G-actin) are polymerized into filamentous actin (F-actin) with a double helical structure, when the concentration of actin is sufficiently high. In the initiation step of actin polymerization, trimeric G-actin works as a filament nucleus since it is much more stable than the G-actin dimer. ATP-actin tends to be incorporated at the end of F-actin, and ATP is rapidly hydrolyzed into ADP and phosphate in the

filamentous form. Many actin-modulating proteins have been identified so far. Profilin is a major one. This protein binds to G-actin and induces ADP-ATP exchange (reviewed by Krishnan and Moens, 2009). Profilin-bound G-actin is able to interact with one end of F-actin, called the “plus end”, but not the “minus end”. Formin is a protein that caps the plus end of F-actin. This actin-modulating protein accelerates actin-nucleation and filament elongation in actin polymerization (reviewed by Goode and Eck, 2007). Formin can associate with profilin-actin at the plus end of F-actin, which enhances the formation of F-actin. On the contrary, cofilin binds to F-actin and severs it (reviewed by Bamburg, 1999). This protein induces F-actin depolymerization from the pointed end. Rapid depolymerization of actin is very important for the cell, because it is indispensable for reorganization of the actin cytoskeleton, which is associated with active cell movement. Several actin-modulating proteins bind to F-actin and produce the three-dimensional structure of the actin cytoskeleton as described below.

Actin cytoskeleton in fission yeast

The fission yeast *Schizosaccharomyces pombe* is an ideal eukaryotic model organism. This unicellular cell is cylindrical about 3 μm in diameter and 8–14 μm long. *S. pombe* cells grow from the cell end(s) in a polarized manner and form a medial septum after they reach a certain length. In fission yeast, three types of the actin cytoskeleton are clearly observed; actin patches, actin cables, and the contractile ring (CR) (reviewed by Kovar et al., 2011). Actin patches are structures that accompany the formation of the

endocytic vesicle on the cell cortex. The Arp2/3-complex, which mimics the trimeric structure of the actin nucleus, induces the organization of short highly branched F-actin. This meshwork structure of F-actin is thought to generate the invagination force of the vesicle. On the contrary, actin cables seem to be a rail for type V myosin-dependent transportation of secretory vesicles. An actin cable is a bundle of longitudinal filaments polymerized by formin For3. Cells lacking functional type V myosin, Myo4/Myo51, or For3 have reduced polarized growth activity (Win et al., 2000; Motegi et al., 2001). The CR is a ring shaped structure in the middle of cell. This actin cytoskeleton contains another fromin Cdc12 and type II myosins, Myo2 and Myo3/Myp2 (Chang et al., 1997; Kitayama et al., 1997; Motegi et al., 1997).

Formation and contraction of the CR

The CR mainly consists of F-actin and type II myosin in *S. pombe*, as well as in animal cells. Contraction of the CR induces formation of a septum in *S. pombe*, whereas it induces ingression of the plasma membrane, called a cleavage furrow, in animal cells. The molecular mechanism of CR formation has been investigated in detail in fission yeast. In this organism, the membrane-anchored Anillin-like protein, Mid1, plays central roles in positioning the CR in the middle of the cell (Sohrmann et al., 1996). Prior to mitosis, 50–60 cortical nodes, a cluster of cytokinetic proteins, are formed at the prospective division site (Vavylonis et al., 2008). The early node contains Mid1 which recruits the scaffold protein Rng2 (a homologue of mammalian IQGAP), type II myosin Myo2, and actin-polymerization factor formin Cdc12 (Laporte et al., 2011). These

nodes interact with each other by mediating F-actin network elongated from each node. In the SCPR (search, capture, pull, and release) model, proposed in the simulation study by Vavylonis et al. (2008), Myo2 exerts its pulling force thorough F-actin, which packs the medial belt of nodes into the ring (Fig. 1; Vavylonis et al., 2008). Namely, new F-actin is polymerized by Cdc12 function in a node and then searches for another node. The filament is captured by Myo2 in another node, and nodes are connected as a network of F-actin. The pulling force of Myo2 closes the other nodes, and releases the filament to capture another filament. Finally, F-actin and the nodes form the single CR. In this process, several actin-bundling proteins are involved in crosslinking F-actin into the ring. F-actin and type II myosin dynamics similar to this model have been proposed for *Xenopus* embryo cytokinesis (Noguchi and Mabuchi, 2001). On the contrary, in fission yeast cells the CR forms prior to nuclear division and it is maintained without contracting before the completion of nuclear division (Alfa et al., 1990), whereas animal cells generally form the CR after nuclear division and immediately enter cytokinesis. It is possible that the CR matures for contraction while nuclear division is occurring. Fission yeast form a septum, which is a cell wall formed in the middle of dividing cell, and the synthetic force of the septum separates the mother cell into two daughter cells (Proctor et al., 2012). It has been shown that one of the most important roles of CR in *S. pombe* is to guide septum formation in the correct direction (Thiyagarajan et al., 2015). Thus, the proper formation and contraction of the CR cooperation with septum synthesis are critical for precise cell division.

Actin-bundling proteins in fission yeast

To date, four actin-bundling proteins, Rng2, Stg1, Fim1, and Ain1 (see below), have been found in *S. pombe*. All of them belong to the calponin superfamily. Calponin is an actin-binding protein that regulates the contraction of skeletal muscle (Rozenblum and Gimona, 2008). It binds to F-actin and inhibits the interaction of myosin with F-actin. A calponin homology (CH) domain is found in the N-terminal region of calponin. Several actin-bundling proteins use a CH domain to bind to F-actin, although, curiously, calponin itself binds to F-actin through its actin-binding sites following the CH domain (Mezqueldi et al., 1992). The calponin family protein IQGAP has a single CH domain at its N-terminal. IQGAPs localize to CR in sea urchin fertilized eggs (Nishimura and Mabuchi, 2003), cultured mammalian cells (Bielak-Zmijewska et al., 2008; Adachi et al., 2014), the budding yeast *Saccharomyces cerevisiae* (Epp and Chant, 1997), and fission yeast (Eng et al., 1998). The IQGAP homolog Rng2 functions as a scaffold protein in the CR of fission yeast. During early mitosis, Mid1 recruits Rng2 to the cortical region of the cell middle. Rng2 arranges F-actin into a single CR (Takaine et al., 2009). The localization of Rng2 depends on its C-terminal domain through interaction with the N-terminal portion of Mid1 (Padmanabhan et al., 2011). On the contrary, the SM22/Transgellin-homologue Stg1, mostly consisting of a single CH domain, localizes to the division site (Nakano et al., 2005). However, Stg1 is not essential for formation of the CR in *S. pombe*.

Several actin-bundling proteins have tandem CH domains as their actin-binding domain (ABD). This type of ABD is found in α -actinin, spectrin, filamin, dystrophin,

ABP-120, and fimbrin. Fimbrin in particular has a double ABD in a single molecule. The Fimbrin-homologue Fim1 localizes to the CR in fission yeast, although it mainly works in cortical actin patches (Nakano et al., 2001; Wu et al., 2001). Double knockout of the genes encoding Fim1 and Ain1, a homologue of α -actinin, causes severe cytokinesis defects in *S. pombe* (Wu et al., 2001). In addition, both Fim1 and Ain1 have a genetic interaction with Rng2. Therefore, these actin-bundling proteins may have overlapping function in cytokinesis. Biochemical studies on Fim1, Stg1, and Rng2 have already been performed (Nakano et al., 2001 and 2005; Takaine et al., 2009). To understand the molecular mechanism of CR formation, I tried to reveal the molecular activity of Ain1 by biochemical, cell biology, and molecular dynamic approaches.

iv. Chapter I

Biochemical and cell biological studies of α -actinin Ain1

Introduction

Cellular function of Ain1

Ain1 is the sole homolog of α -actinin in fission yeast. A previous study showed that *ain1⁺* gene deletion abrogated cell division only under stress conditions like in medium containing 1 M KCl and at the low temperature of 18 °C (Wu et al., 2001). Moreover, the $\Delta ain1$ allele showed synthetic defects with other mutant alleles including actin *act1*, profilin *cdc3*, IQGAP *rng2*, and anillin-like *mid1* (Wu et al., 2001). In addition, simultaneous deletion of both *ain1⁺* and *fim1⁺* is synthetically lethal (Wu et al., 2001), suggesting that actin-bundling activity is essential for cell viability. On the contrary, overproduction of *ain1⁺* induces CR deformation, which leads to abnormal cytokinesis (Laporte et al., 2012). Laporte et al. have also proposed, using mathematical simulation, that proper bundling activity is needed to correctly form the CR (Laporte et al., 2012).

Of the four actin-bundling proteins in *S. pombe*, only Ain1 and Rng2 specifically localize to the CR. These proteins do not localize to other types of actin cytoskeleton such as actin patches and actin cables. What molecular mechanisms allow them to distinguish F-actin in the CR from other actin cytoskeletons? It has been demonstrated that Ain1 localization depends on F-actin (Wu et al., 2001), whereas the interaction between the C-terminus of Rng2 and the N-terminus of Mid1 is important for the CR-localization of Rng2 (Padmanabhan et al., 2011). In addition, a truncated Rng2 protein consisting of only a CH domain associates with all of the actin cytoskeletons in fission yeast cells (Takaine et al., 2009). Cells lacking Rng2 with a CH domain do not show significant cytokinesis defects (Tebbs and Pollard, 2013). These results suggested

that actin-binding may be a subsidiary function in Rng2. As mentioned above, Ain1 and Rng2 may have redundant roles in CR. Therefore, it is possible that Ain1 may play an important role in bundling F-actin in CR during cytokinesis.

Functional domains in Ain1

Ain1 consists of three functional domains, an N-terminal ABD, spectrin repeats (SPR) in the middle region of the molecule, and a C-terminal EF-hand. As mentioned above, the ABD consists of two CH domains, CH1 and CH2. Ain1 is believed to form an anti-parallel dimer via SPR as well as other α -actinin. Of note, its SPR is two repeats whereas mammalian α -actinins have four repeats in their SPRs (Virel and Backman, 2007). The EF-hand is one of the well characterized protein domains which contain calcium-binding motifs. It has been reported Ca^{2+} ion suppresses the actin-binding activity of mammalian α -actinins (Jayadev et al., 2012). On the contrary, the essential residues for Ca^{2+} -binding are not conserved in Ain1, suggesting that the EF-hand of Ain1 cannot bind to the calcium ions (Wu et al., 2001). However, their interaction has not been elucidated yet. In addition, there has not been a biochemical and structural analysis of Ain1. Here I investigated the biochemical properties and the mechanism of Ain1's CR-specific localization. Actin-binding and actin-bundling activities were measured using recombinant proteins. Moreover, I investigated the functional importance of each domain in Ain1 by using point mutated or truncated proteins.

Materials and Methods

Yeast strains and cell cultures

S. pombe wild-type ($h^- leu1-32$) and $\Delta ain1$ ($h^- \Delta ain1::kan^r$) were inoculated from our laboratory stock for use in this study. To visualize F-actin, a strain that expressed LifeAct peptide with four tandem fluorescent protein ($h^- ura4$ -D18 *ade6*-M216 *leu1::cdc4*-promoter-*lifeact*-4xmCherry) was also used. The rich medium YE (0.5 % Yeast Extract (Becton and Dickinson (BD)), 3% D-glucose (Wako), and 2% Bacto Agar (BD)) and minimal medium EMM were used for all cell cultures.

Plasmid and DNA construction

The *ain1⁺* gene was artificially synthesized and cloned into a bacterial plasmid. The plasmid was digested with the restriction enzymes EcoRI and SalI and the *ain1⁺* gene was subcloned in the GST-fused protein expressing vector pGEX6P-1 (GE Healthcare (GE)). To observe N-terminal YFP-tagged Ain1 in yeast, the *ain1⁺* gene was subcloned into the thiamine-repressive vector pREP1 (Maundrell, 1993). The truncated or point mutated genes were prepared using a PrimeSTAR mutagenesis basal kit (Takara). Cells were transformed with plasmids by the lithium acetate method (Suga and Hatakeyama, 2005). Transformed cells were auxotrophically selected on EMM plates with the appropriate amino acids.

Protein purification

The *E. coli* BL21 strain was transformed with the protein-expressing vector. The resultant *E. coli* transformants were cultured in LB medium with 100 µg/mL of ampicillin at 36 °C. Early logarithmic phase cells were induced to express the GST-fused protein by adding 0.1 mM IPTG to the cell culture. After 4 hours, the cells were harvested and stored in a -80 °C freezer. Frozen cells were sonicated in the lysis buffer (50 mM Tris-HCl (pH8.0), 100 mM NaCl, 0.5% NP-40, 1 mM DTT, 2 mM PMSF, and 1 µg/ml Pepstatin A), and the cell lysate was centrifuged (10,000 × g, 10 min). The supernatant was incubated with Glutathione Sepharose 4B beads (GE) at 4 °C for 18 hours. The GST-fused protein was cleaved with PreScission Protease (GE) in P buffer (50 mM Tris-HCl (pH 6.8), 150 mM NaCl, 1 mM DTT, and 1 mM EDTA), and the elution was stored at -80 °C.

The rabbit or chicken skeletal muscle G-actin was kindly provided by Prof. Uyeda's lab (National Institute of Advanced Industrial Science and Technology). G-actin was polymerized in KMEI buffer (100 mM imidazole-HCl pH 7.5, 100 mM KC, 1mM MgCl₂, 0.2 mM EGTA, 0.2 mM DTT, and 0.2 mM ATP).

Co-sedimentation assay

Different concentrations of Ain1 recombinant proteins were mixed with F-actin in KMEI buffer, and incubated at 25 °C for 30 min. To evaluate the effect of Ca²⁺, CaCl₂ was added to the mix at a final concentration of 0.2 mM. The mixture was centrifuged at 200,000 × g for 20 min (high-speed), or 15,000 × g for 15 min (low-speed). The

supernatant and pellet were run on SDS-PAGE and stained with Coomassie brilliant blue. The stained gels were scanned into digital images and analyzed with the ImageJ software (Schneider et al., 2012). To calculate the K_d value, hyperbolic curve fitting was executed on the R software (<https://www.R-project.org>).

Actin-bundling assay

The microtubes were dried with methanol dissolved rhodamine-phalloidin and then dissolved in the KMEI buffer to label F-actin with rhodamine-phalloidin. The labeled F-actin and recombinant proteins were mixed together and incubated at 25 °C for 10 min. A BX51 fluorescence microscope (Olympus) with a PlanApo 100x/1.40NA objective lens (Olympus) was used for the observations. Microscopic images were obtained using a cooled charge-coupled device (CCD) camera, (ORCAII-ER-1394, Hamamatsu Photonics) with Simple PCI software (Compix Inc.).

Cellular localization of Ain1

For microscopic observation of cells containing the pREP1 vector, 5 μ M thiamine was added to the EMM medium to repress its expression. In this condition, small amounts of the gene product are produced because of the leakiness of the repression. For induction, thiamine was removed from the cell culture and cells were further incubated for more than 20 hours. The fluorescent images were acquired with the microscopy system described in the previous section.

Western blot

Cell extracts were prepared using the NaOH method (Kushnirov, 2000; Matsuo et al., 2006). The SDS-PAGE gels were transferred to a PVDF membrane. The YFP or GFP-tagged proteins were then probed using the primary antibody (1/1000 anti-GFP mouse-IgG, (Roche)) overnight at 4 °C, and the secondary antibody (1/5000 anti-mouse IgG HRP-conjugated goat-IgG (Santa Cruz Biotechnology)) for 2 hours at the room temperature. The chemiluminescence with ELC Prime (GE) was detected using the EZ-Capture MG scanning system (ATTO).

Results

Ain1 binds weakly to F-actin

To begin studying the biochemical activities of Ain1, the recombinant proteins Ain1FL (full-length), Ain1FL R216E, Ain1 Δ EF, and Ain1 ABD were expressed in *E. coli* and purified (Fig. 5). First, the binding-affinity of Ain1FL for F-actin was measured. Ain1FL mostly appeared in the supernatant with high-speed ultracentrifugation (Fig. 6), while the F-actin precipitated in the pellet fraction because of its apparent molecular weight. The amount of Ain1FL in the pellet was slightly increased with the addition of F-actin. The dissociation constant (K_d) of the Ain1FL and F-actin was calculated from the proportion of Ain1FL in the supernatant and pellet (Fig. 7). The K_d of Ain1FL was $6.53 \pm 0.55 \mu\text{M}$ (mean \pm SD). Although, an excess of Ain1 was added and each data point fit nicely on the curve the fitted curve did not reach a plateau. This K_d is close to the value of $4.3 \mu\text{M}$ estimated in an independent study (Li et al., 2016). The K_d of other actin-bundling proteins had already been measured in fission yeast; Stg1, $4.4 \mu\text{M}$ (Nakano et al., 2005); Rng2CHD, $0.21 \pm 0.08 \mu\text{M}$ (Takaine et al., 2009); Fim1, $0.645 \pm 0.15 \mu\text{M}$ (Skau et al., 2011). The higher K_d value of Ain1FL than the other actin-bundling proteins indicated that Ain1FL binds weakly to F-actin.

Next, I attempted to measure the actin-binding affinity of Ain1 ABD. However, this was not possible since the amount of Ain1 ABD in the pellet fraction did not change regardless of the existence of F-actin.

It has been reported that a K255E mutation in human α -actinin ACTN4 induces the familial disease, focal segmental glomerulosclerosis (Kaplan et al., 2000; Weins et

al., 2005, 2007). This mutation could cause a conformational change in ABD and increase its affinity for F-actin. The homologous mutation R216E was introduced into Ain1 (Ain1 FL R216E), and the biochemical features of Ain1 FL R216E were examined. The K_d of Ain1 FL R216E was $1.80 \pm 0.47 \mu\text{M}$ (mean \pm SD) (Fig. 7). This suggests that the R216E mutation greatly increases actin-binding activity. Ain1 FL R216E also formed thick but short actin filaments (Fig. 8). The bundling-activity was linearly increased along with the addition of Ain1 FL R216E (Fig. 10). The strong binding affinity of Ain1 FL R216E might induce inefficient cross-linking.

Ain1 bundles F-actin into long and thick filaments

The actin-bundling activity of Ain1 was measured using rhodamine-phalloidin labeled F-actin (Fig. 8). Without Ain1, F-actin formed short and thin filaments. On the contrary, in the presence of Ain1FL it formed long and thick filaments. In addition, I carried out low-speed ($15,000 \times g$) co-sedimentation assays for Ain1 with F-actin. In this assay, there was hardly non-bundled F-actin in the pellet fraction (Fig. 9). Precipitated F-actin increased with increasing Ain1FL (Fig. 10). Taken together, I concluded that Ain1 was able to bundle F-actin *in vitro*.

In contrast, bundled filaments were not observed with Ain1 ABD (Fig. 8, 9, 10). Note that the pellet of Ain1 ABD increased when the concentration was zero. This might be due to non-specific binding to microtubes and is consistent with the high speed co-sedimentation assay of ABD with F-actin.

Different functions of the two CH domains.

To investigate the role of Ain1's functional domains, the cellular localization of Ain1 and the truncated proteins were observed (Fig. 11). Two dots were observed with Ain1FL indicating that it formed a sharp CR as demonstrated by a previous study (Wu et al., 2001). On the contrary, Ain1 ABD did not localize to any major actin structures. This is consistent with my previously mentioned biochemical assay results. Interestingly, expression of CH1 alone, namely the N-terminal half of the Ain1 ABD, labeled the major actin cytoskeletons (Fig. 11). Moreover, overexpression of CH1 induced the formation of thick F-actin bundles in fission yeast cells (Fig. 15). This bundle was not destroyed by treatment with the actin-depolymerization drug latrunculin A (Lat-A), suggesting its abnormal stability. On the contrary, the C-terminal half of Ain1 ABD, CH2 alone, did not localize to any actin structures (Fig. 11). However, Ain1ΔCH1, which lacks CH1, localized to the CR though its signal is weak (Fig. 11). Overexpressed Ain1ΔCH1 localized to the nucleus in wild-type cells where it produced a multinuclear phenotype (Fig. 12). Both CH domains seem to possess actin-binding ability, although isolated Ain1 ABD was not able to bind to F-actin. Thus, it is possible that the two CH domains might have a suppressive relationship in ABD.

By analogy with mammalian α -actinin, I found three actin-binding sites (ABSs) in Ain1. CH1 has two ABSs; ABS1 (VQNRTFTKWFNTKL, 9–22 a. a.) and ABS2 (LTNIGPADIVDGNLKLILGLIWTLLIR, 86–112 a. a.), while CH2 has a single ABS, ABS3 (LTAKEGLLLWCQRKT, 123–137 a. a.). To investigate this in detail, charged or hydrophilic residues on the ABSs were substituted with alanine, and the mutant

proteins were expressed *in vivo*. It was found that Ain1 FL ABS1-2A (Q10A, T13A) localized to the CR and that Ain1 CH1 ABS1-2A labeled all the major actin structures in fission yeast (Fig. 11). Thus, ABS1 is not necessary for the cellular localization of Ain1. In contrast, neither Ain1 FL ABS2-1A (K100A) nor Ain1 CH1 ABS2-1A localized to any actin cytoskeleton, suggesting that ABS2 is essential for actin-binding of Ain1 *in vivo*. In addition, ABS3-2A mutation (R135A, K136A) abrogated the CR-localization of Ain1ΔCH1. Thus, ABS3 probably functions as the sole ABS in the CH2. Moreover, I found that Ain1 FL ABS3-2A localized not only to the CR but also formed dots at the cell tip (Fig. 11). Hence, ABS3 has a crucial role in CR-specific localization of Ain1.

My biochemical study revealed that the human disease-related point mutation R216E on Ain1 enhanced actin-binding activity *in vitro*. It was found that Ain1 FL R216E affected CR formation; the mutant protein localized to an abnormal branched CR (Fig. 11). This phenotype was similar to that seen with the overexpression of Ain1 (Laporte et al., 2012). To evaluate the accumulation of the proteins on the CR, the ratios of the fluorescent intensity of YFP-tagged proteins in the CR vs. the cytosol were measured (Fig. 13). Ain1 FL R216E abundantly accumulated on the CR (7.39 ± 3.01 , mean \pm SD) compared to the wild-type (3.78 ± 0.92). I then investigated the possibility that the R216E mutation altered the actin-binding roles of ABS1 and ABS2 through changing the conformation of ABD. The simultaneous Ain1 ABS2-1A R216E mutant localized to the CR (Fig. 11). On the contrary, Ain1 ABS1-2A R216E did not appear in any actin structures (Fig. 11). This result supported the possibility that the R216E

mutation might switch the importance of the two ABSs by changing the configuration of the ABD.

Next, I examined the functional ability of the Ain1 mutants through complementation assays using $\Delta ain1$ cells in a stress condition. A previous study showed that $\Delta ain1$ was not able to grow at 18 °C in the presence of 1 M potassium chloride (Wu et al., 2001). The wild-type and $\Delta ain1$ cells expressing Ain1 FL or Ain1 FL ABS3-2A were able to form colonies under the stress condition (Fig. 16). Artificial localization of Ain1 to other actin structures is unlikely to affect cell growth ability. On the contrary, Ain1 FL R216E partially rescues the viability of $\Delta ain1$. Neither Ain1 ABS1-2A nor Ain1 ABS2-1A could complement a gene deletion defect in $ain1^+$. Coincidentally, $\Delta ain1$ expressing Ain1 ΔCH1 was not able to grow in the same condition. These results suggest that the ability to localize to the CR is essential for the function of Ain1.

The EF-hand is essential to the cellular localization

As mentioned above, fission yeasts have several types of actin cytoskeletons i.e. actin patches, actin cable, and the CR. Ain1 only localizes to the CR. However, the mechanism of this preference had not yet been uncovered. EF-hand is one of the Ca^{2+} dependent regulatory motifs (Ikura, 1996). The two right-angled α -helices and loop in the EF-hand motif capture Ca^{2+} . There are many examples of the EF-hand motif altering the conformation and function of a protein by binding Ca^{2+} (Chazin, 2011). In mammalian cells, some types of α -actinin have calcium ion-sensitive EF-hand motifs

(Foley and Young, 2014). The actin-binding affinity of α -actinin is decreased in the presence of Ca^{2+} (Jayadev et al., 2012). Moreover, it has been suggested that Ca^{2+} binding is required for the recruitment of α -actinin in the cleavage furrow in mammalian cultured cells (Jayadev et al., 2012). To investigate the function of the EF-hand and calcium ions in Ain1, I tested the biochemical and cellular properties of Ain1 Δ EF, which lacks the C-terminal EF-hand (Fig. 7). The K_d of Ain1 Δ EF was $4.92 \pm 1.08 \mu\text{M}$ (mean \pm SD). This value is not much different from Ain1 FL. In the bundling assay, Ain1 Δ EF formed thick actin filaments (Fig. 8), although the bundling-activity saturated at lower concentrations than Ain1FL (Fig. 10). Moreover, Ain1 FL bundled F-actin even in the presence of an excess concentration of Ca^{2+} (Fig. 10). These results suggest that the actin-bundling activity of Ain1 is not affected by Ca^{2+} .

However, interestingly, I found that Ain1 Δ EF failed to localize to the CR or any other actin cytoskeleton (Fig. 11). This is not due to the level of protein expression; the expression from the plasmid of both Ain1 FL and Ain1 Δ EF were similar (Fig. 14A). To further confirm this delocalization, I compared strains in which C-terminal GFP-tagged Ain1 or Ain1 Δ EF were expressed from the *ain1*⁺ locus, to ensure that they had the same expression pattern (Fig. 14A, B). Similar to N-terminal YFP-tagged proteins, Ain1 Δ EF-GFP did not appear in the middle of the cell (Fig. 14C). Moreover, Ain1 Δ EF could not rescue the viability of Δ *ain1* cells under the stress condition (Fig. 16). Therefore, I concluded that the EF-hand motif played an important role in cellular the localization of Ain1 to the CR. It is likely that in an antiparallel Ain1 dimer each EF-hand, which is adjacent to the ABD in the partner molecule, controls the

actin-binding activity of its partner *in vivo*. An *In vitro* study previously performed on the human skeletal α -actinin ACTN4 showed that the EF-hand seems to regulate actin-binding activity (Noegel et al., 1987). In addition, I found that Ain1 Δ EF with the R216E mutation localized to the CR, cortical dots, and thin filaments in an unspecific manner (Fig. 11). The inter-molecular interaction of EF-hand and ABD might be needed for CR-specific localization of *S. pombe* Ain1.

PIP₂ is unlikely to regulate Ain1

Phosphatidylinositol 4,5-bisphosphate (PIP₂) binds to α -actinin, and increases the actin-bundling activity of α -actinin (Fukami et al., 1994, 1996). The PIP₂ binding-site is conserved with Ain1 sharing 47% identity with chicken skeletal muscle α -actinin (Wu et al., 2001). PI(4)P-5 kinase Its3, produces PIP₂ and localizes to the division site in *S. pombe* cells. The temperature-sensitive mutant *its3-1* showed disorganized actin patches with high temperatures because of its kinase activity (Zhang et al., 2000). Ain1 localized to the middle of the cell at both normal and high temperatures (Fig. 17). No other structures except the CR were observed. Thus, PIP₂ might not be involved in Ain1 regulation.

Discussion

Ain1 modulates F-actin dynamics in the CR

My biochemical study revealed that Ain1 bundles F-actin and that it has a weaker affinity for F-actin than other actin-bundling proteins. In mammalian cells, α -actinin, which functions in cytokinesis, has a higher affinity for F-actin ($K_d = 0.20 \pm 0.01 \mu\text{M}$) (Low et al., 2010). The size of the cells could account for the difference in their affinity for F-actin. Mammalian cells have a large and broad CR proportional to their cell size and α -actinin needs to tightly bundle F-actin in the CR. On the contrary, fission yeasts have a small CR and F-actin seems to assemble in the CR probably without a particularly strong bundling step during the SCPR process (see General introduction). Nevertheless, Ain1 is necessary as a redundant bundler. During CR formation, actin filaments are moved by the motor activity of the type II myosin, Myo2. If the filaments are too tightly bundled, they cannot move. In a previous study, a mathematical simulation demonstrated that excessive crosslinking causes deformation of the CR (Laporte et al., 2012). In this study, it was shown that cells expressing Ain1 R216E had impaired CR formation (Fig. 11). The effective gathering of F-actin into the CR may be affected in those cells.

It has been reported that mammalian α -actinin decreases the constriction rate of the CR (Mukhina et al., 2007). On the contrary, the constriction rate is not altered by the presence of Ain1 (Laporte et al., 2012), suggesting that Ain1 may not regulate the construction of CR in a negative manner. I demonstrated that Ain1 had high a K_d for

F-actin. The weak affinity of Ain1 may ensure the proper constriction of the CR in fission yeast.

Mechanism of CR-specific localization of Ain1

I showed that the actin-bundling activity of Ain1 was not affected by the presence of Ca^{2+} (Fig. 10). In addition, Ain1 ΔEF was able to bind to F-actin almost equally as well as Ain1 FL (Fig. 7). Interestingly, I found that the Ain1 ΔEF failed to localize the CR. A structural study of human α -actinin revealed that the EF-hand interacts with the ABD and the neck region which is located between the ABD and SPR (Ribeiro et al., 2014). Despite the lack of calcium sensitivity, the EF-hand might ensure the formation of the functional dimer *in vivo*. This difference in the necessity of the EF-hand for F-actin-binding of Ain1 *in vivo* and *in vitro* may be explained by the structural properties of F-actin. *In vitro*, F-actin is forced to polymerize by increasing ion concentrations and becomes stable filaments. On the contrary, F-actin dynamically turns over *in vivo*, and several actin-modulating proteins decorate the filament. EF-hand may change the structure of the ABD in the paired molecule to make the ABD suitable for actin-binding *in vivo*. The EF-hand regulatory mechanism is worth studying in the future.

I succeeded in demonstrating the unspecific localization of Ain1 CH1 (Fig. 11) by expressing truncated proteins. In addition, I demonstrated that CH2 plays an important role in the CR-specific localization of Ain1 (Fig. 11). Another actin-bundling protein, Rng2, has a single CH domain in the N-terminus, Rng2CHD. The truncated Rng2CHD

is observed in the three types of actin structures. On the contrary, Rng2CHD with the C-terminal region localizes specifically to the CR (Takaine et al., 2009). These studies suggest that the region following CH1 may regulate the specificity of CH1.

In addition, Ain1 CH2 may favor F-actin decorated with CR-specific actin-binding proteins. Tropomyosin Cdc8, an F-actin side-binding protein, is one of the candidates. In *S. pombe*, Cdc8 mainly localizes to the CR (Balasubramanian et al., 1992). Studies have demonstrated the importance of post-translational modification of Cdc8 for the cellular localization; non-acetylated Cdc8 localizes to actin patches, whereas N-terminal-acetylated Cdc8 only localizes to the CR (Coulton et al., 2010; Johnson et al., 2014). A recent study demonstrated that the actin binding-affinity of Ain1 increases when Cdc8 decorates F-actin (Christensen et al., 2019). It is possible that CH2 interacts directly with Cdc8 or recognizes the surface of F-actin modulated by Cdc8. In addition, it has been reported that Cdc8 appears on the CR after CR formation (Wu et al., 2010). During the formation of the CR, before Cdc8 decorates the F-actin, Ain1 may bundle F-actin with a weak affinity, which would ensure that the F-actin in the CR is dynamic. After the CR formation, the presence of Cdc8 might increase Ain1's binding affinity for CR actin. In *S. pombe*, CR needs to be prevented from constricting until the end of nuclear division. Ain1 and Cdc8 may stiffen the F-actin bundle in the CR during this maintenance period (Fig. 18). Thus, Ain1 may be a molecule that monitors the state of F-actin in the CR. It is also speculated that Ain1 may alter its activity depending on the structural and mechanical state of F-actin.

Acknowledgements

I am deeply grateful to Professor Kentaro Nakano for his insightful guidance and continuous encouragement. I would like to thank Associate Professors Hidekazu Kuwayama, Ryuhei Harada, and Yousuke Degawa for reading this thesis and their meaningful discussions. I express my gratitude to Professor Taro QP Uyeda (Waseda University) for kindly providing the purified actin and helpful advice. I am grateful to Assistant Professor Masak Takaine (Gumma University Initiative for Advanced Research, GIAR), and Professor Osamu Numata for their valuable comments.

References

- Adachi, M., Kawasaki, A., Nojima, H., Nishida, E., and Tsukita, S. (2014) Involvement of IQGAP family proteins in the regulation of mammalian cell cytokinesis. *Genes Cells.* **19**, 803–820
- Addario, B., Sandblad, L., Persson, K., and Backman, L. (2016) Characterisation of *Schizosaccharomyces pombe* α -actinin. *PeerJ.* **4**, e1858
- Alfa, C., and Hyams, J. (1990) Distribution of tubulin and actin through the cell division cycle of the fission yeast *Schizosaccharomyces japonicus* var. *versatilis*: a comparison with *Schizosaccharomyces pombe*. *J. Cell. Sci.* **96**, 71–77
- Balasubramanian, M.K., Helfmant, D.M., and Hemmingsen, S.M. (1992). A new tropomyosin essential for cytokinesis in the fission yeast. *Nature* **360**, 84–87.
- Bamburg, J. R. (1999) Proteins of the ADF/Cofilin Family: Essential Regulators of Actin Dynamics. *Annu. Rev. Cell Dev. Biol.* **15**, 185–230
- Bielak-Zmijewska, A., Agnieszka, K., Katarzyna, S., Marek, M., and Borsuk, E. (2008) Cdc42 protein acts upstream of IQGAP1 and regulates cytokinesis in mouse oocytes and embryos. *Dev. Biol.* **322**, 21–32
- Bonafé, N., Chaussepied, P., Capony, J. P., Derancourt, J., and Kassab, R. (1993) Photochemical cross-linking of the skeletal myosin head heavy chain to actin subdomain-1 at Arg95 and Arg28. *Eur. J. of Biochem.* **213**, 1243–1254

- Chang, F., Drubin, D., and Nurse, P. (1997) cdc12p, a Protein Required for Cytokinesis in Fission Yeast, Is a Component of the Cell Division Ring and Interacts with Profilin. *J Cell Biol.* **137**, 169–182
- Chazin, W. J. (2011) Relating Form and Function of EF-Hand Calcium Binding Proteins. *Acc. Chem. Res.* **44**, 171–179
- Childers, M. C., and Daggett, V. (2017) Insights from molecular dynamics simulations for computational protein design. *Mol. Syst. Des. Eng.* **2**, 9–33
- Christensen, J. R., Homa, K. E., Morganthaler, A. N., Brown, R. R., Suarez, C., Harker, A. J., O'Connell, M. E., and Kovar, D. R. (2019) Cooperation between tropomyosin and α -actinin inhibits fimbrin association with actin filament networks in fission yeast. *Cell Bioloy.* **8**, e47279
- Conde, C., and Cáceres, A. (2009) Microtubule assembly, organization and dynamics in axons and dendrites. *Nat. Rev. Neurosci.* **10**, 319–332
- Coulton, A. T., East, D. A., Agnieszka, G. R., Lehman, W., and Mulvihill, D. P. (2010) The recruitment of acetylated and unacetylated tropomyosin to distinct actin polymers permits the discrete regulation of specific myosins in fission yeast. *J. Cell. Sci.* **123**, 3235–3243
- Durrant, J. D., and McCammon, J. A. (2011) Molecular dynamics simulations and drug discovery. *BMC Biol.* **9**, 1–9
- Eng, K., Naqvi, N., Wong, K., and Balasubramanian, M. (1998) Rng2p, a protein required for cytokinesis in fission yeast, is a component of the actomyosin ring and the spindle pole body. *Curr. Biol.* **8**, 611–621

- Epp, J., and Chant, J. (1997) An IQGAP-related protein controls actin-ring formation and cytokinesis in yeast. *Curr. Biol.* **7**, 921–929
- Foley, K. S., and Young, P. W. (2014) The non-muscle functions of actinin: an update. *Biochem. J.* **459**, 1–13
- Fukami, K., Endo, T., Imamura, M., and Takenawa, T. (1994) alpha-Actinin and vinculin are PIP2-binding proteins involved in signaling by tyrosine kinase. *J. Biol. Chem.* **269**, 1518–1522
- Fukami, K., Sawada, N., Endo, T., and Takenawa, T. (1996) Identification of a phosphatidylinositol 4,5-bisphosphate-binding site in chicken skeletal muscle alpha-actinin. *J. Biol. Chem.* **271**, 2646–2650
- Galkin, V. E., Orlova, A., VanLoock, M. S., Rybakova, I. N., Ervasti, J. M., and Egelman, E. H. (2002) The utrophin actin-binding domain binds F-actin in two different modes: implications for the spectrin superfamily of proteins. *J. Cell Biol.* **157**, 243–251
- Galkin, V., Orlova, A., Salmazo, A., Kristina, D.-C., and Egelman, E. (2010) Opening of tandem calponin homology domains regulates their affinity for F-actin. *Nat. Struct. Mol. Biol.* **17**, 614–616
- Goode, B. L., and Eck, M. J. (2007) Mechanism and Function of Formins in the Control of Actin Assembly. *Annu. Rev. Biochem.* **76**, 593–627
- Herrmann, H., Bär, H., Kreplak, L., Strelkov, S. V., and Aebi, U. (2007) Intermediate filaments: from cell architecture to nanomechanics. *Nat. Rev. Mol. Cell Biol.* **8**, 562–573

- Hertig, S., Latorraca, N. R., and Dror, R. O. (2016) Revealing Atomic-Level Mechanisms of Protein Allostery with Molecular Dynamics Simulations. *PLOS Comp. Biol.* **12**, e1004746
- Hollingsworth, S. A., and Dror, R. O. (2018) Molecular Dynamics Simulation for All. *Neuron*. **99**, 1129–1143
- Ikura, M. (1996). Calcium binding and conformational response in EF-hand proteins. *Trends Biochem. Sci.* **21**, 14–17.
- Jayadev, R., Kuk, C., Low, S., and Maki, M.-H. (2012) Calcium sensitivity of α -actinin is required for equatorial actin assembly during cytokinesis. *Cell Cycle*. **11**, 1929–1937
- Johnson, M., East, D. A., and Mulvihill, D. P. (2014) Formins determine the functional properties of actin filaments in yeast. *Curr. Biol.* **24**, 1525–1530
- Kaplan, J., Kim, S., North, K., Rennke, H., Correia, L., Tong, H., Mathis, B., JC, R.-P., Allen, P., Beggs, A., and Pollak, M. (2000) Mutations in ACTN4, encoding alpha-actinin-4, cause familial focal segmental glomerulosclerosis. *Nat. Genet.* **24**, 251–256
- Keep, N. H., Winder, S. J., Moores, C. A., Walke, S., Norwood, F. L., and Kendrick-Jones, J. (1999) Crystal structure of the actin-binding region of utrophin reveals a head-to-tail dimer. *Structure*. **7**, 1539–1546
- Kelley, L. A., Mezulis, S., Yates, C. M., Wass, M. N., and Sternberg, M. J. E. (2015) The Phyre2 web portal for protein modeling, prediction and analysis. *Nat. Protoc.* **10**, 845–858

- Kitayama, C., Sugimoto, A., and Yamamoto, M. (1997) Type II Myosin Heavy Chain Encoded by the *myo2* Gene Composes the Contractile Ring during Cytokinesis in *Schizosaccharomyces pombe*. *J. Cell Biol.* **137**, 1309–1319
- Krishnan, K., and Moens, P. D. J. (2009) Structure and functions of profilins. *Biophys. Rev.* **1**, 71–81
- Kovar, D. R., Sirotnik, V., and Lord, M. (2011) Three's company: the fission yeast actin cytoskeleton. *Trends Cell Biol.* **21**, 177–187
- Kuhlman, P. A., Hemmings, L., and Critchley, D. R. (1992) The identification and characterisation of an actin-binding site in α -actinin by mutagenesis. *FEBS Lett.* **304**, 201–206
- Kushnirov, V. (2000) Rapid and reliable protein extraction from yeast. *Yeast*. **16**, 857–860
- Laporte, D., Coffman, V. C., Lee, I.-J. J., and Wu, J.-Q. Q. (2011) Assembly and architecture of precursor nodes during fission yeast cytokinesis. *J. Cell Biol.* **192**, 1005–1021
- Laporte, D., Ojkic, N., Vavylonis, D., and Wu, J.-Q. Q. (2012) α -Actinin and fimbrin cooperate with myosin II to organize actomyosin bundles during contractile-ring assembly. *Mol. Biol. Cell.* **23**, 3094–3110
- Lebart, M.-C., Mbjean, C., Casanova, D., Audemard, E., Derancourt, J., Roustan, C., and Benyamin, Y. (1994) Characterization of the Actin Binding Site on Smooth Muscle Filamin. *J. Biol. Chem.* **269**, 4279–4284

- Lehman, W., Craig, R., Kendrick-Jones, J., and Sutherland-Smith, A. J. (2004) An open or closed case for the conformation of calponin homology domains on F-actin? *J Muscle Res Cell Motil.* **25**, 351–358
- Levine, B. A., Moir, A. J. G., Patchell, V. B., and Perry, S. V. (1990) The interaction of actin with dystrophin. *FEBS Lett.* **263**, 159–162
- Li, Y., Christensen, J. R., Homa, K. E., Hocky, G. M., Fok, A., Sees, J. A., Voth, G. A., and Kovar, D. R. (2016) The F-actin bundler α -actinin Ain1 is tailored for ring assembly and constriction during cytokinesis in fission yeast. *Mol. Biol. Cell.* **27**, 1821–1833
- Loncarek, J., and Bettencourt-Dias, M. (2018) Building the right centriole for each cell type. *J. Cell Biol.* **217**, 823–835
- Love, D. R., Hill, D. F., Dickson, G., Spurr, N. K., Byth, B. C., Marsden, R. F., Walsh, F. S., Edwards, Y. H., and Davies, K. E. (1989) An autosomal transcript in skeletal muscle with homology to dystrophin. *Nature.* **339**, 55–58
- Low, S. H., Mukhina, S., Srinivas, V., Ng, C. Z., and Maki, M.-H. (2010) Domain analysis of alpha-actinin reveals new aspects of its association with F-actin during cytokinesis. *Exp. Cell Res.* **316**, 1925–1934
- Matsuo, Y., Asakawa, K., Toda, T., and Katayama, S. (2006) A Rapid Method for Protein Extraction from Fission Yeast. *Biosci. Biotech. Biochem.* **70**, 1992–1994
- Maundrell, K. (1993) Thiamine-repressible expression vectors pREP and pRIP for fission yeast. *Gene.* **123**, 127–130

- McGough, A., Pope, B., Chiu, W., and Weeds, A. (1997) Cofilin Changes the Twist of F-Actin: Implications for Actin Filament Dynamics and Cellular Function. *J. of Cell Biol.* **138**, 771–781
- Meunier, S., and Vernos, I. (2012) Microtubule assembly during mitosis – from distinct origins to distinct functions? *J. Cell Sci.* **125**, 2805–2814
- Mezgueldi, M., Fattoum, A., Derancourt, J., and Kassab, R. (1992) Mapping of the Functional Domains in the Amino-terminal Region of Calponin. *J. Biol. Chem.* **267**, 15943–15951
- Moores, C. A., and Kendrick-Jones, J. (2000) Biochemical characterisation of the actin-binding properties of utrophin. *Cell Motil. and the Cytoskeleton.* **46**, 116–128
- Motegi, F., Nakano, K., Kitayama, C., Yamamoto, M., and Mabuchi, I. (1997) Identification of Myo3, a second type-II myosin heavy chain in the fission yeast *Schizosaccharomyces pombe*. *FEBS Lett.* **420**, 161–166
- Motegi, F., Arai, R., and Mabuchi, I. (2001) Identification of Two Type V Myosins in Fission Yeast, One of Which Functions in Polarized Cell Growth and Moves Rapidly in the Cell. *Mol Biol Cell.* **12**, 1367–1380
- Mukhina, S., Wang, Y., and Maki, M.-H. (2007) α -Actinin Is Required for Tightly Regulated Remodeling of the Actin Cortical Network during Cytokinesis. *Dev. Cell.* **13**, 554–565
- Nakajima, J., Noguchi, T. Q. P., Nagasaki, A., Tokuraku, K., and Uyeda, T. Q. P. (2016) Allosteric regulation by cooperative conformational changes of actin filaments drives mutually exclusive binding with cofilin and myosin. *Scientific Reports.* **6**, 1–11

- Nakano, K., Bunai, F., and Numata, O. (2005) Stg 1 is a novel SM22/transgelin-like actin-modulating protein in fission yeast. *FEBS Lett.* **579**, 6311–6
- Nakano, K., Satoh, K., Morimatsu, A., Ohnuma, M., and Mabuchi, I. (2001). Interactions among a fimbrin, a capping protein, and an actin-depolymerizing factor in organization of the fission yeast actin cytoskeleton. *Mol. Biol. Cell.* **12**, 3515–3526.
- Ngo, K. X., Kodera, N., Katayama, E., Ando, T., and Uyeda, T. Q. (2015) Cofilin-induced unidirectional cooperative conformational changes in actin filaments revealed by high-speed atomic force microscopy. *eLife.* **4**, e04806
- Ngo, K. X., Umeki, N., Kijima, S. T., Kodera, N., Ueno, H., Furutani-Umezu, N., Nishimura, Y., and Mabuchi, I. (2003) An IQGAP-like protein is involved in actin assembly together with Cdc42 in the sea urchin egg. *Cell Motil. Cytoskeleton.* **56**, 207–218
- Noegel, A., Witke, W., and Schleicher, M. (1987) Calcium-sensitive non-muscle α -actinin contains EF-hand structures and highly conserved regions. *FEBS Lett.* **221**, 391–396
- Noguchi, T., Arai, R., Motegi, F., Nakano, K., and Mabuchi, I. (2001). Contractile Ring Formation in *Xenopus* Egg and Fission Yeast. *Cell Structure and Function* **26**, 545–554.
- Padmanabhan, A., Bakka, K., Sevugan, M., Naqvi, N. I., D’souza, V., Tang, X., Mishra, M., and Balasubramanian, M. K. (2011) IQGAP-related Rng2p organizes cortical nodes and ensures position of cell division in fission yeast. *Curr. Biol.* **21**, 467–472

- Proctor, S. A., Minc, N., Boudaoud, A., and Chang, F. (2012) Contributions of Turgor Pressure, the Contractile Ring, and Septum Assembly to Forces in Cytokinesis in Fission Yeast. *Curr. Biol.* **22**, 1601–1608
- Ribeiro, E. de A., Pinotsis, N., Ghisleni, A., Salmazo, A., Konarev, P. V., Kostan, J., Sjöblom, B., Schreiner, C., Polyansky, A. A., Gkougkoulia, E. A., Holt, M. R., Aachmann, F. L., Zagrović, B., Bordignon, E., Pirker, K. F., Svergun, D. I., Gautel, M., and Kristina, D.-C. (2014) The structure and regulation of human muscle α -actinin. *Cell*. **159**, 1447–1460
- Rozenblum, G. T., and Gimona, M. (2008) Calponins: adaptable modular regulators of the actin cytoskeleton. *Int. J. Biochem. Cell Biol.* **40**, 1990–1995
- Schneider, C. A., Rasband, W. S., and Eliceiri, K. W. (2012) NIH Image to ImageJ: 25 years of image analysis. *Nat. Methods*. **9**, 671–675
- Shams, H., Golji, J., Garakani, K., and Mofrad, M. R. (2016) Dynamic Regulation of α -Actinin's Calponin Homology Domains on F-Actin. *Biophys. J.* **110**, 1444–1455
- Skau, C. T., Courson, D. S., Bestul, A. J., Winkelman, J. D., Rock, R. S., Sirotkin, V., and Kovar, D. R. (2011) Actin filament bundling by fimbrin is important for endocytosis, cytokinesis, and polarization in fission yeast. *J. Biol. Chem.* **286**, 26964–26977
- Sohrmann, M., Fankhauser, C., Brodbeck, C., and Simanis, V. (1996) The *dmf1/midl* gene is essential for correct positioning of the division septum in fission yeast. *Genes Dev.* **10**, 2707–2719

- Suga, M., and Hatakeyama, T. (2005) A rapid and simple procedure for high-efficiency lithium acetate transformation of cryopreserved *Schizosaccharomyces pombe* cells. *Yeast.* **22**, 799–804
- Sutherland-Smith, A. J., Moores, C. A., Norwood, F. L. M., Hatch, V., Craig, R., Kendrick-Jones, J., and Lehman, W. (2003) An Atomic Model for Actin Binding by the CH Domains and Spectrin-repeat Modules of Utrophin and Dystrophin. *J. Mol. Biol.* **329**, 15–33
- Takaine, M., Numata, O., and Nakano, K. (2009) Fission yeast IQGAP arranges actin filaments into the cytokinetic contractile ring. *EMBO J.* **28**, 3117–3131
- Tebbs, I. R., and Pollard, T. D. (2013) Separate roles of IQGAP Rng2p in forming and constricting the *Schizosaccharomyces pombe* cytokinetic contractile ring. *Mol. Biol. Cell.* **24**, 1904–1917
- Thiyagarajan, S., Munteanu, E.L., Arasada, R., Pollard, T.D., and O'Shaughnessy, B. (2015). The fission yeast cytokinetic contractile ring regulates septum shape and closure. *J. Cell Sci.* **128**, 3672–3681.
- Varland, S., Vandekerckhove, J., and Drazic, A. (2019) Actin Post-translational Modifications: The Cinderella of Cytoskeletal Control. *Trends Biochem. Sci.* **44**, 502–516
- Vavylonis, D., Wu, J.-Q. Q., Hao, S., Ben, O., and Pollard, T. D. (2008) Assembly mechanism of the contractile ring for cytokinesis by fission yeast. *Science.* **319**, 97–100
- Virel, A., and Backman, L. (2007) A comparative and phylogenetic analysis of the alpha-actinin rod domain. *Mol. Biol. Evol.* **24**, 2254–2265

- Vivo, D., M., Masetti, M., Bottegoni, G., and Cavalli, A. (2016). Role of Molecular Dynamics and Related Methods in Drug Discovery. *J. Med. Chem.* **59**, 4035–4061.
- Weins, A., Kenlan, P., Herbert, S., Le, T. C., Villegas, I., Kaplan, B. S., Appel, G. B., and Pollak, M. R. (2005) Mutational and biological analysis of α -actinin-4 in focal segmental glomerulosclerosis. *J. Am. Soc. Nephrol.* **16**, 3694–3701
- Weins, A., Schlondorff, J. S., Nakamura, F., Denker, B. M., Hartwig, J. H., Stossel, T. P., and Pollak, M. R. (2007) Disease-associated mutant alpha-actinin-4 reveals a mechanism for regulating its F-actin-binding affinity. *Proc. Natl. Acad. Sci. U.S.A.* **104**, 16080–16085
- Win, T. Z., Gachet, Y., Mulvihill, D. P., May, K. M., and Hyams, J. S. (2000) Two type V myosins with non-overlapping functions in the fission yeast Schizosaccharomyces pombe: Myo52 is concerned with growth polarity and cytokinesis, Myo51 is a component of the cytokinetic actin ring. *J. of Cell Sci.* **111**, 69–79
- Winder, S. J., Hemmings, L., Maciver, S. K., Bolton, S. J., Tinsley, J. M., Davies, K. E., Critchley, D. R., and Kendrick-Jones, J. (1995) Utrophin actin binding domain: analysis of actin binding and cellular targeting. *J. Cell Sci.* **108**, 63–71
- Wu, J., Bähler, J., and Pringle, J. (2001) Roles of a fimbrin and an alpha-actinin-like protein in fission yeast cell polarization and cytokinesis. *Mol. Biol. Cell.* **12**, 1061–1077
- Zhang, Y., Sugiura, R., Lu, Y., Asami, M., Maeda, T., Itoh, T., Takenawa, T., Shuntoh, H., and Kuno, T. (2000) Phosphatidylinositol-4-Phosphate 5-Kinase Its3 and Calcineurin Ppb1 Coordinately Regulate Cytokinesis in Fission Yeast. *J. Biol. Chem.* **275**, 35600–35606

ix. Figures

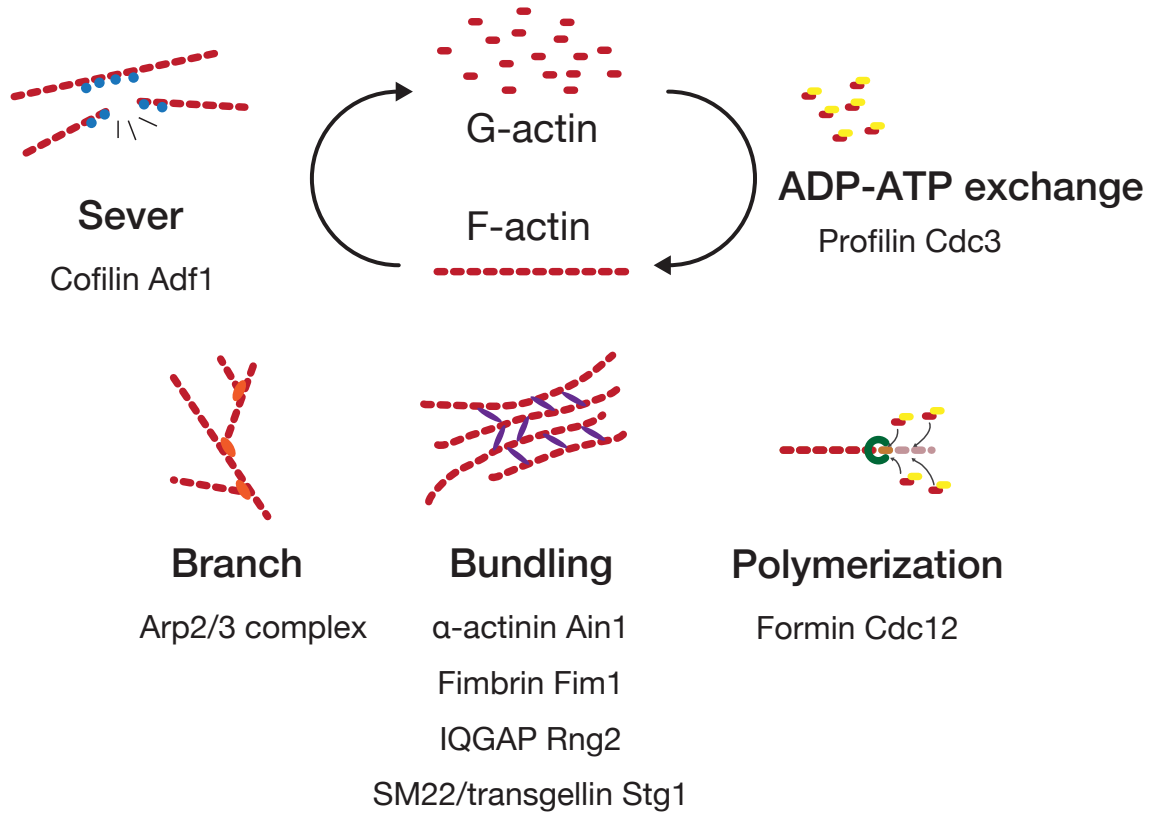


Figure 1 Actin modulating proteins in fission yeast

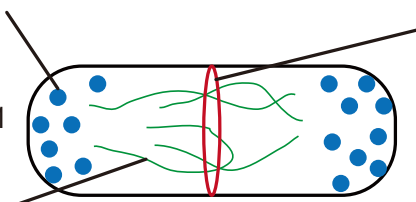
The actin modulating proteins involved in the turnover of G-actin and F-actin are illustrated.

Actin patch

Fimbrin Fim1

SM22/Transgelin Stg1

Actin cable



Contractile Ring

α -Actinin Ain1

IQGAP Rng2

SM22/Transgelin Stg1

Fimbrin Fim1

Figure 2 Actin cytoskeletons in fission yeast

The actin cytoskeletons in fission yeast are illustrated. The CR (red), actin patches (blue), and actin cable (green). The actin-bundling proteins are listed according to where they localize.

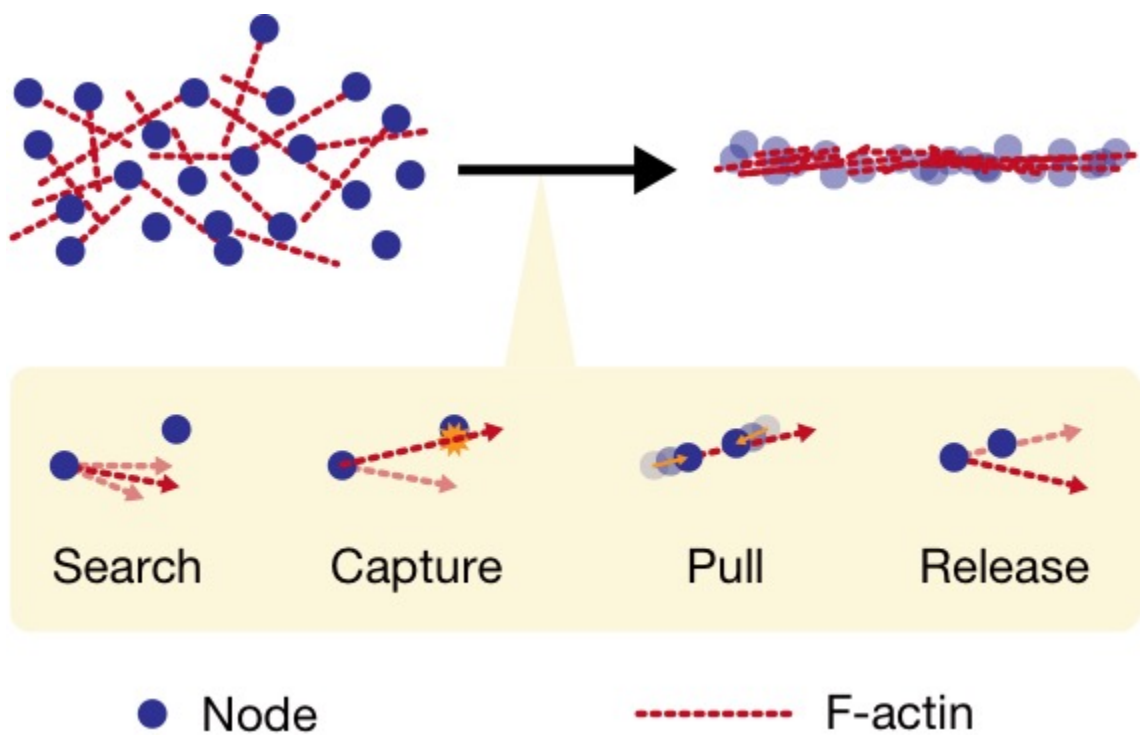


Figure 3 The SCPR model of CR formation

The SCPR model is illustrated. The actin filament (red line) elongates from the node (blue circle).

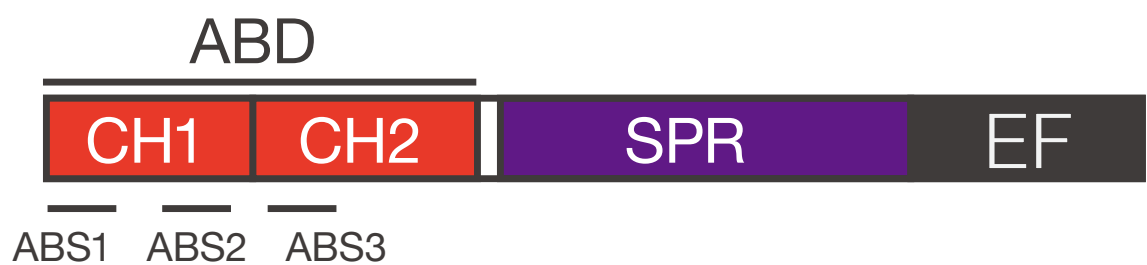


Figure 4 Functional domains of Ain1

The functional domains of Ain1 are illustrated. The CH1 and CH2 (red), SPR (purple), and EF (gray) are shown.

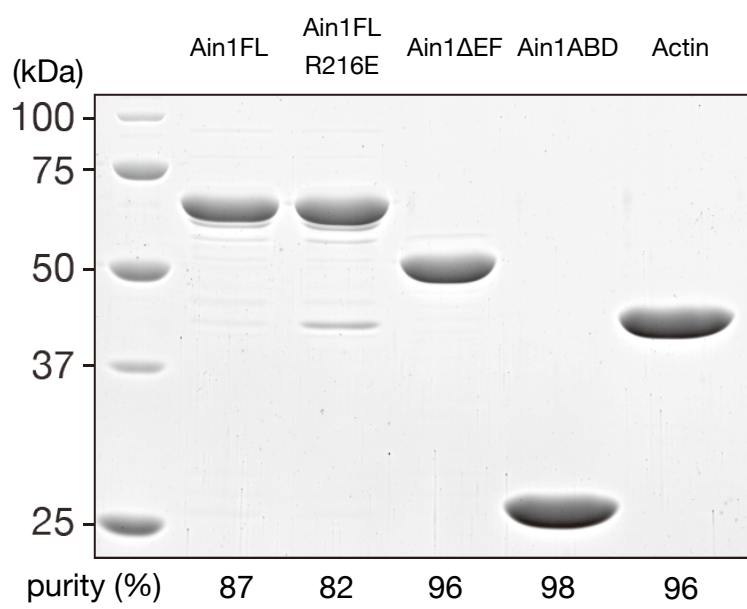


Figure 5 Purification of recombinant proteins.

Purified Ain1 FL (72.4 kDa), Ain1 FL R216E (72.4 kDa), Ain1 Δ EF (57.3 kDa), Ain1ABD (26.7kDa), and actin were run to an SDS-PAGE. The gel was stained with CBB and purities were measured. Two-microgram of proteins were applied in each lane.

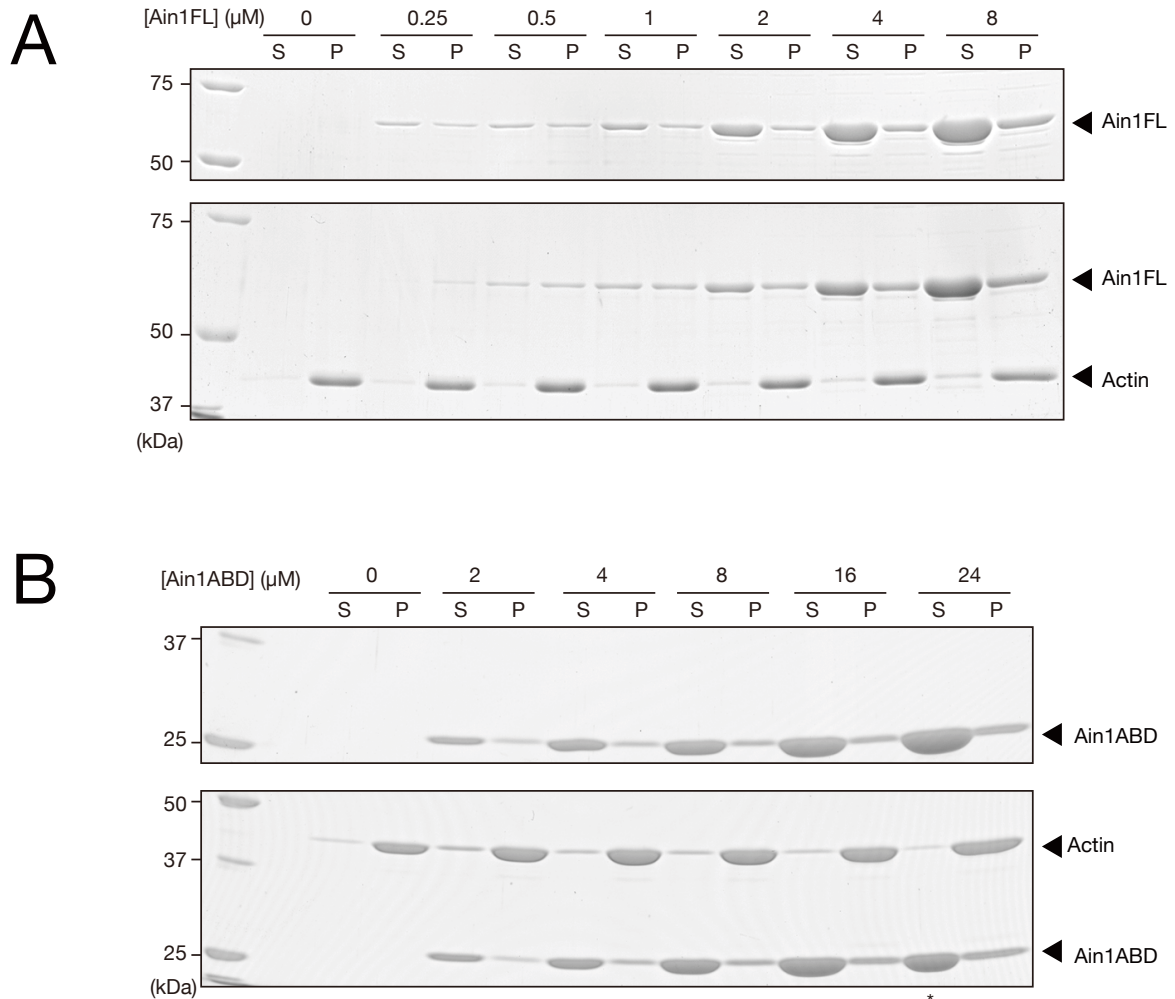


Figure 6 High-speed co-sedimentation of Ain1 with F-actin

(A) High-speed co-sedimentation of Ain1FL (0.25–8 μ M) with (bottom) or without F-actin (2 μ M) (top). The supernatant (S) and pellet (P) were subjected to the SDS-PAGE and stained by CBB. (B) High-speed co-sedimentation of the Ain1ABD (2–24 μ M) with (bottom) or without (top) F-actin (4 μ M). Half amounts of the supernatant were applied on the lane indicated with an asterisk.

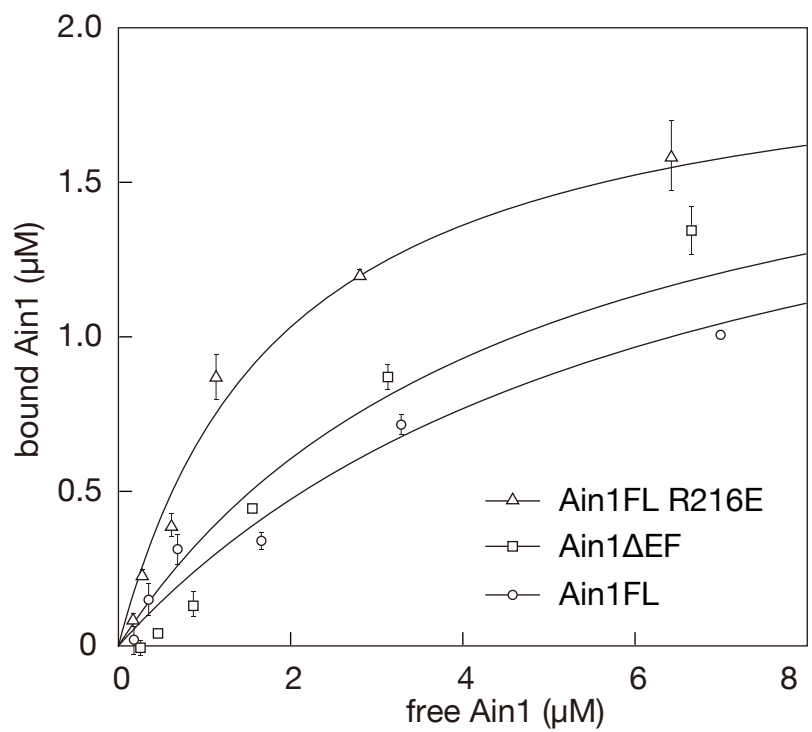


Figure 7 Calculation of the dissociation constants

The free protein (x-axis) and actin-bound protein (y-axis) are plotted (Ain1 FL, circle; Ain1 Δ EF, square; Ain1 FL R216E, triangle). Three independent high-speed co-sedimentation experiments were performed. Each data points is the average of three experiments with their SD. The data series were fitted to hyperbolic curves. The coefficients of these curves are the apparent dissociation constants.

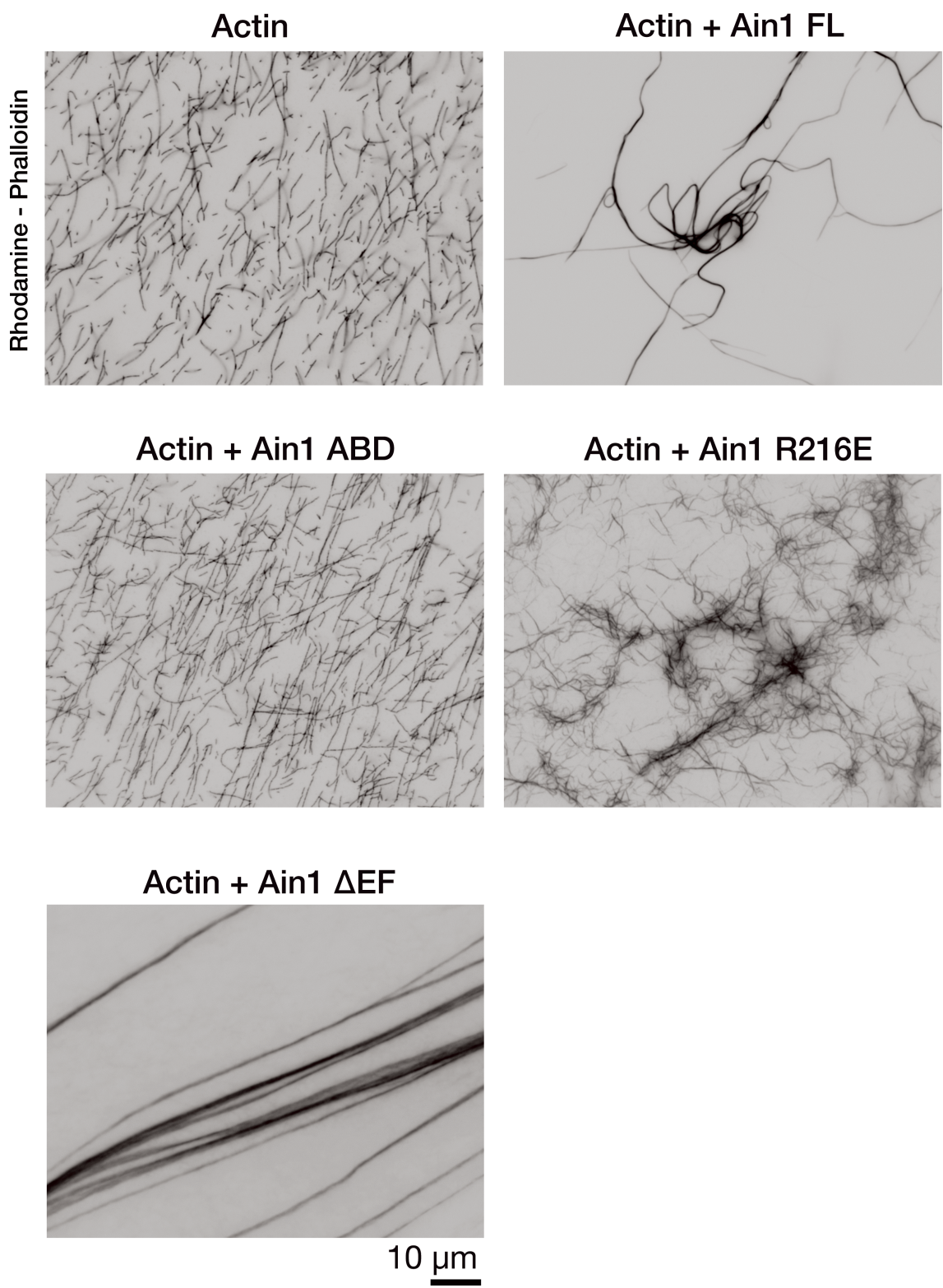


Figure 8 Ain1 bundling of F-actin

Fluorescent images of rhodamine-phalloidin labeled actin (4 μ M) were taken with and without Ain1 proteins (8 μ M). The images were inverted and converted to grayscale. The bar is 10 μ m. Ain1 FL and Ain1 Δ EF formed long and thick filaments. Ain1 FL R216E formed short and aggregated filaments.

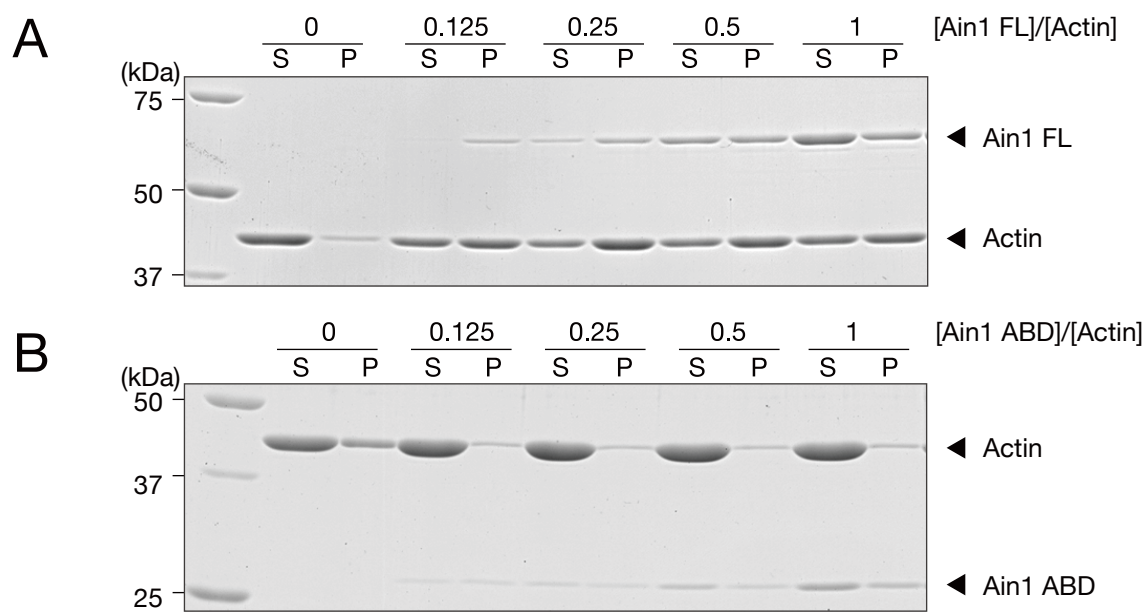


Figure 9 Low-speed co-sedimentation of Ain1 with F-actin

Low-speed co-sedimentation of Ain1 (A) or Ain1 ABD (B) (0.25–2 μ M) with F-actin (2 μ M) were performed. The supernatant (S) and pellet (P) were subjected to SDS-PAGE and stained by CBB.

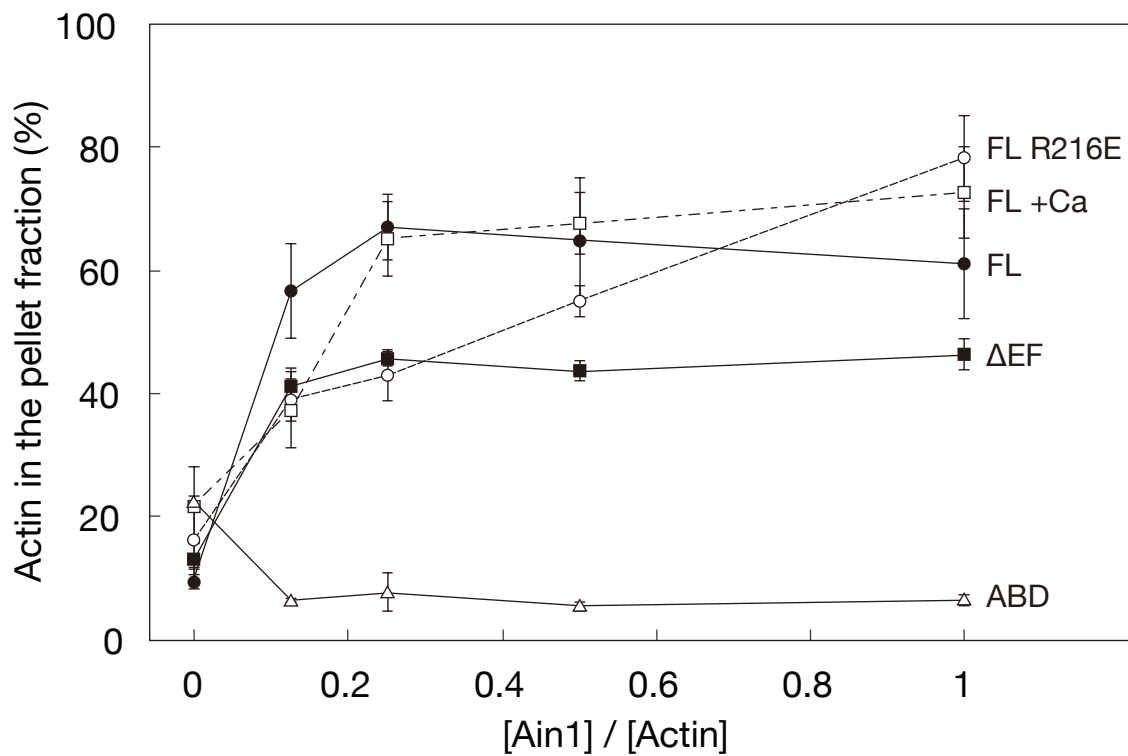


Figure 10 Bundling activities of Ain1

The pellet fractions of the Ain1 from the low-speed co-sedimentation assay are plotted.

Three independent experiments were performed (mean \pm SD). Ain1 FL (black circle),

Ain1 FL +Ca (white square), and Ain1 Δ EF (black square) reached a plateau. Ain1 FL

R216E (white circle) showed a linear increase.

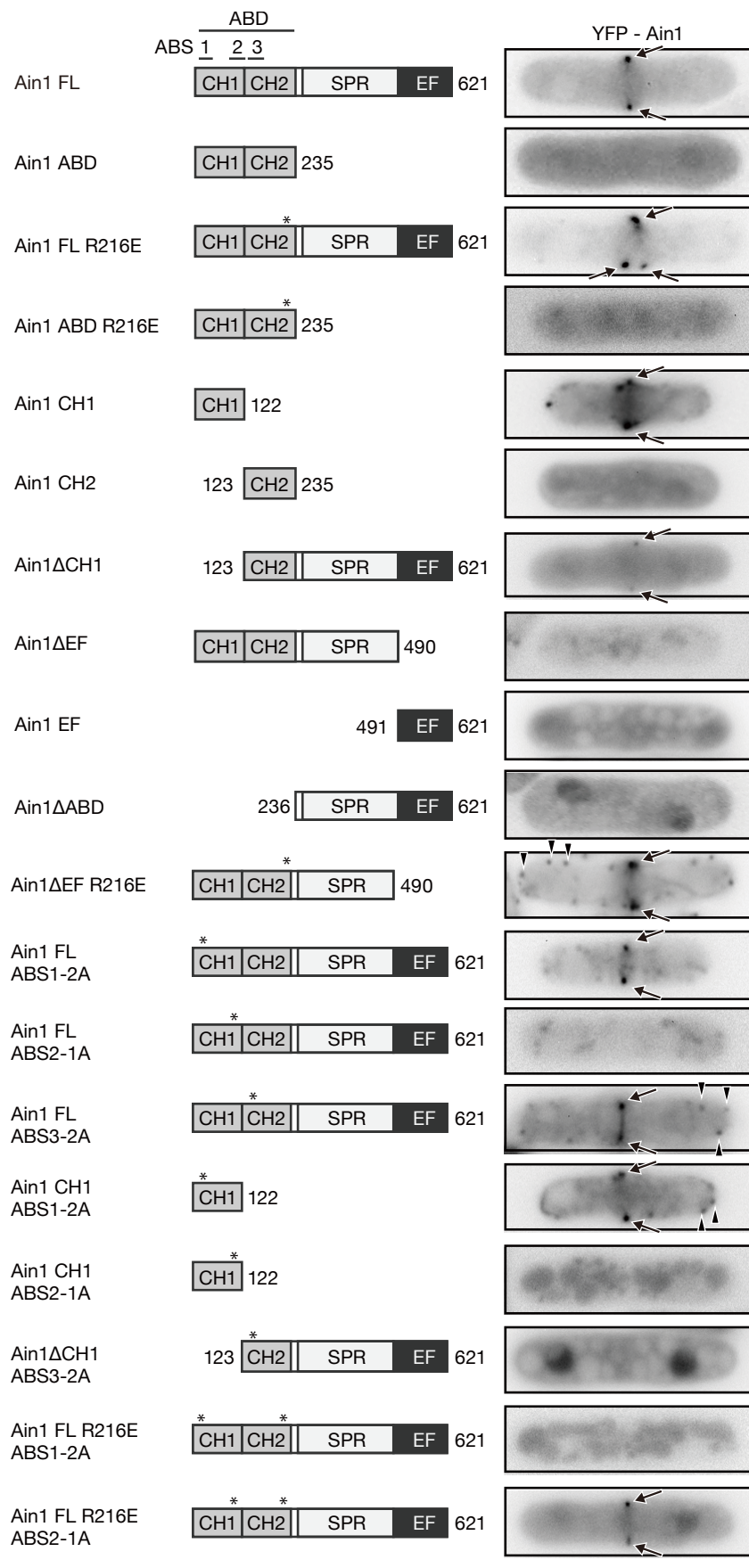


Figure 11 Cellular localization of Ain1

Localization of YFP-tagged Ain1 proteins were observed in the wild-type cells. Thiamine (final conc. 5 μM) was added to the EMM medium and truncated Ain1 were expressed under the repressive condition. Their representative localizations in the mitotic cells are shown. The numbers at the side of primary structures indicate the terminal positions of the residues. The asterisks indicate the point mutations of R216E, ABS1-2A, ABS2-1A, and ABS3-2A. Images were inverted and converted into grayscale. The arrows indicate the CR, and arrowheads indicate cortical actin dots. The bar is 10 μm.

YFP-Ain1 Δ CH1 induced

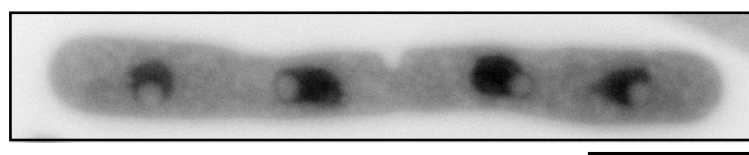


Figure 12 Overexpression of Ain1ΔCH1 induced multinuclear cells

Ain1ΔCH1 was overexpressed in the wild-type cell and accumulated in the nuclear crescent. The bar is 10 μm .

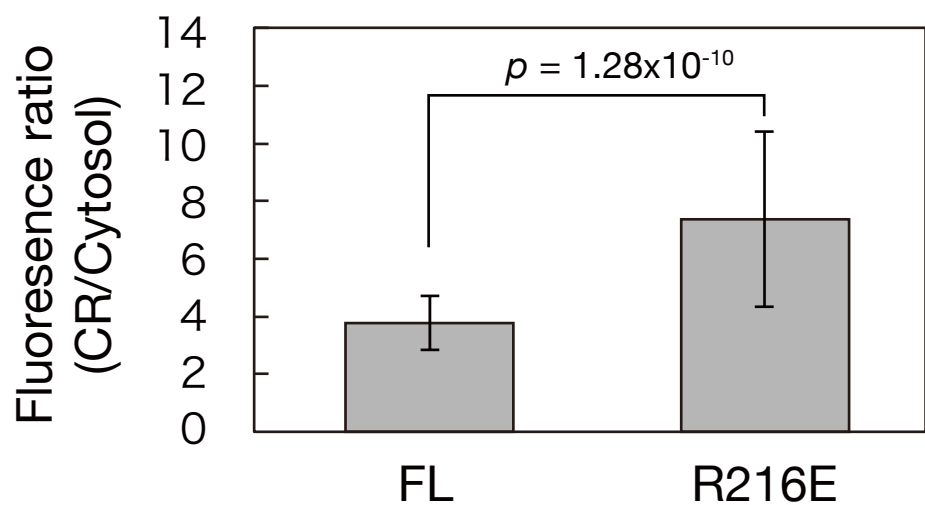


Figure 13 Accumulation of Ain1 on the CR

The ratios of the fluorescent intensity from Ain1 FL and Ain1 FL R216E in the CR and cytosol were measured. A two-tailed Student's *t*-test was performed assuming unequal variance.

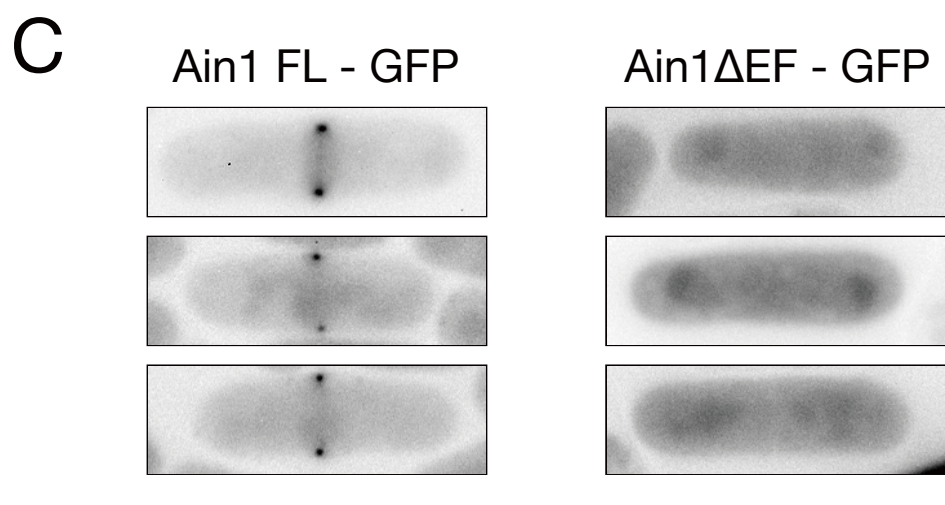
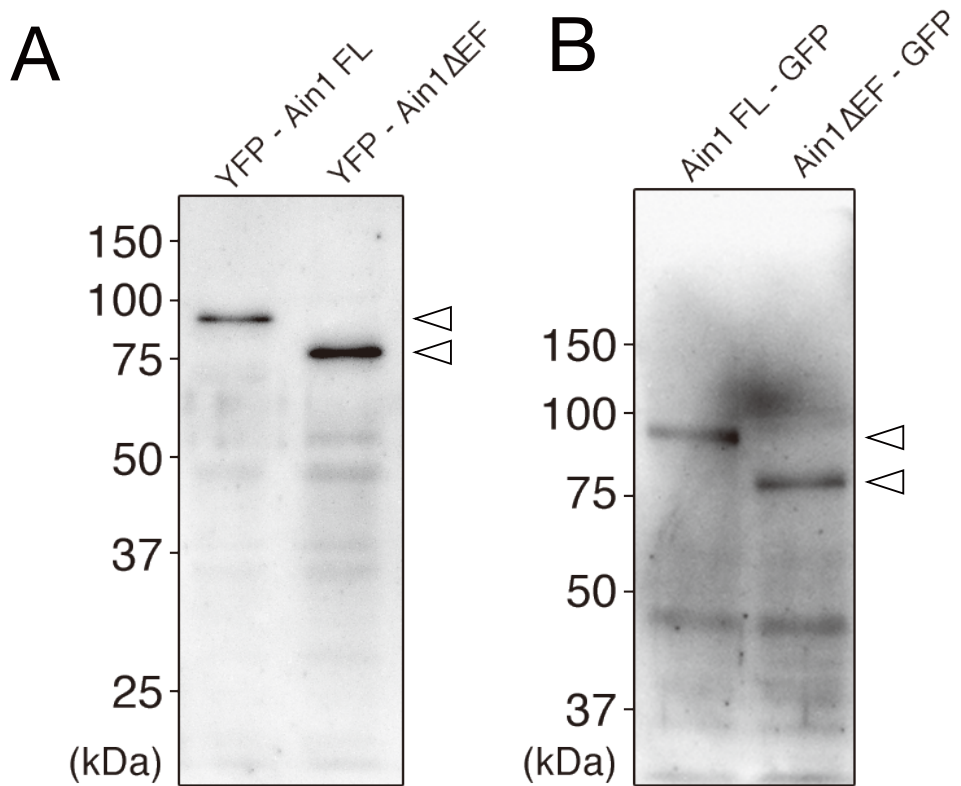


Figure 14 Expression level and localization of Ain1 and Ain1ΔEF

(A) A comparison of the expression level of YFP-Ain1 FL and YFP-Ain1ΔEF. The lysates of the wild-type cell expressing YFP-Ain1 FL or YFP-Ain1ΔEF from the pREP1 plasmid were separated on an SDS-PAGE and detected using α -GFP antibody.

(B) The experiment was performed as in (A) but endogenous Ain1 FL-GFP and Ain1ΔEF-GFP expressing cells were used. (C) Cellular localization of Ain1 FL-GFP and Ain1ΔEF-GFP in the wild-type cell. Images were inverted and converted into the grayscale. The bar is 10 μ m.

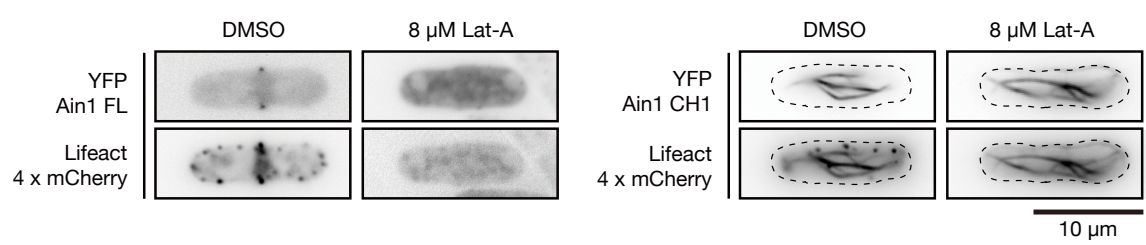


Figure 15 Ain1 CH1 formed thick filaments

The localization of Ain1 FL and Ain1 CH1 in lifeact-4xmCherry cells. Treatment with 8 μ M Lat-A disrupted the cortical dots, however thick filaments remained with the Ain1 CH1. Images were inverted and converted into grayscale. The bar is 10 μ m.

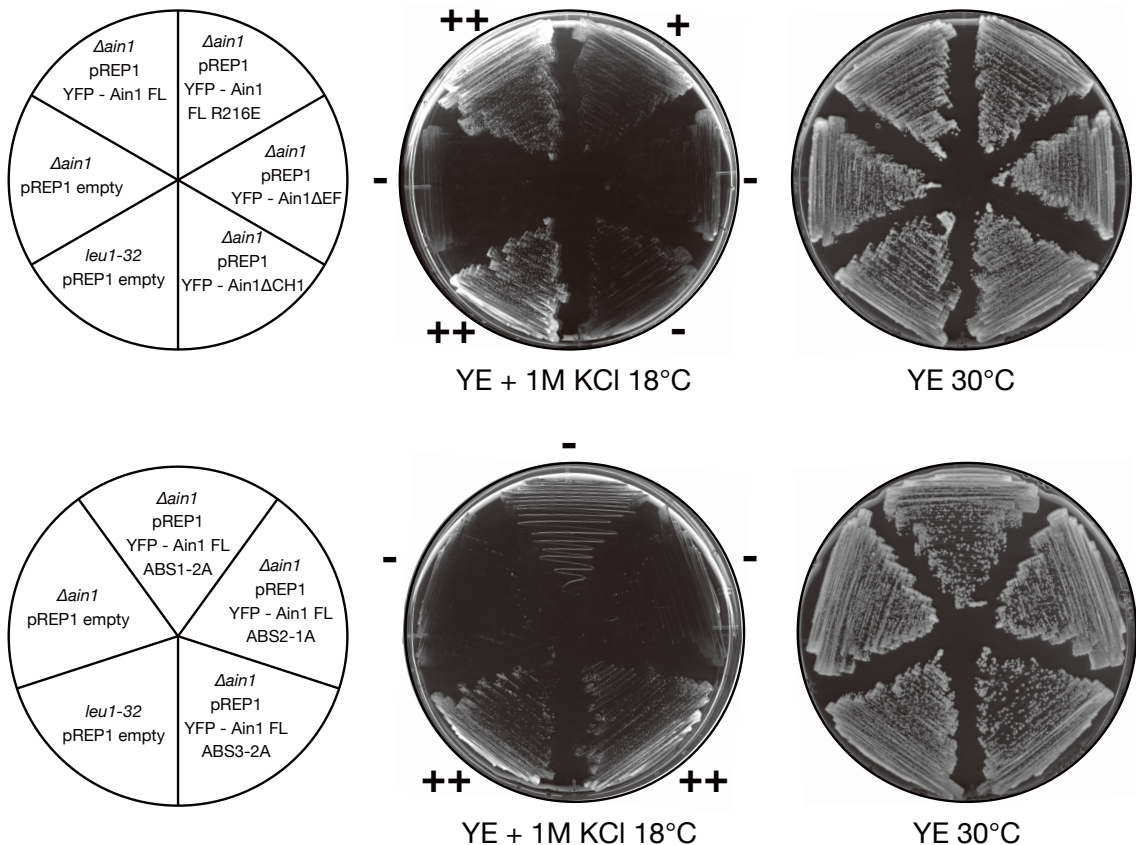
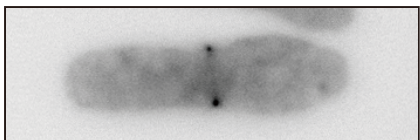


Figure 16 Functional complementation of Ain1 mutants

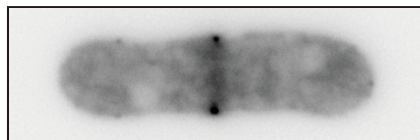
The wild-type and *ain1*-null cells with pREP1 vectors were incubated on a YE plate at 30 °C for 3 days (right) or YE containing 1M potassium chloride at 18 °C for a week (left). The growth of the cells are indicated; ++, normal-sized colonies; +, small colonies; -, no colony.

its3 YFP - Ain1

25°C



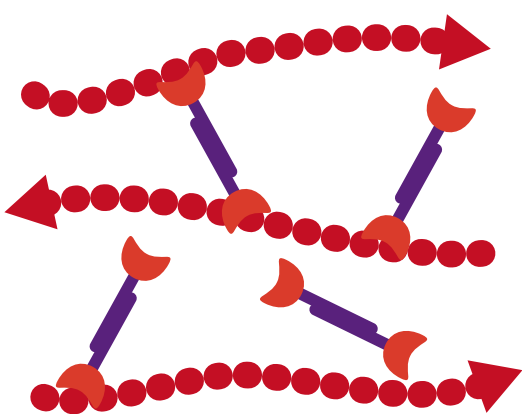
36°C



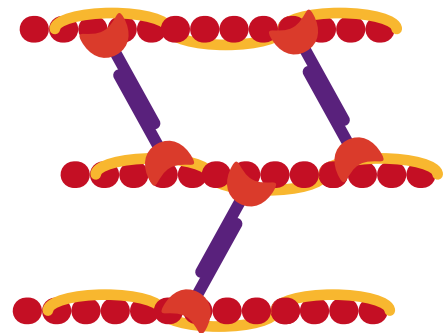
10 μm

Figure 17 Ain1 localized to the CR in the *its3-1* mutant

The *its3-1* cells expressing YFP-Ain1 FL at 25 °C (permissive temperature) or 36 °C (restrictive temperature). Ain1 localized to the cell middle of the cells at both temperatures. Images were inverted and converted into grayscale. The bar is 10 µm.



Non-decorated filaments
in the formation of the CR



Cdc8-decorated filaments
in the maintenance of the CR

Figure 18 Schematic illustration of Ain1 in each phase of the CR lifespan

During CR-formation (left), F-actin is newly polymerized in the cell middle. Ain mildly bundles them into the CR. During CR-maintenance (right), acetylated-Cdc8 joins in the CR. Ain1 increases its actin-binding activity and holds the CR tightly.